

Light Stops and Fine-Tuning in MSSM

Ali Çiçi^{a,1}, Zerrin Kırca^{a,2} and Cem Salih Ün^{a,3}

^a*Department of Physics, Uludağ University, TR16059 Bursa, Turkey*

Abstract

We discuss the fine-tuning issue within the MSSM framework. Following the idea that the fine-tuning can measure effects of some missing mechanisms we impose non-universal gaugino masses at the GUT scale, and explore the low scale implications. We consider the stop mass with a special importance and consider the mass scales which are excluded by the LHC experiments. We find that the stop mass can be as light as 200 GeV, while the mass scales below this scale are excluded by the experimental constraints imposed in our analyses. After discussing the fine-tuning and its implications, we consider detection of stop quarks at LHC over some benchmark points which yield stop masses in a range 200-700 GeV. Even though the LHC constraints are severe and they exclude this mass scales for the stop quark, we show that the stops can still escape from detection, when the model is restricted from the GUT scale.

¹E-mail: 501507007@ogr.uludag.edu.tr

²E-mail: zkirca@uludag.edu.tr

³E-mail: cemsalihun@uludag.edu.tr

1 Introduction

The Standard Model (SM) of elementary particles is one of the most successful theory in physics, which has been tested and confirmed by the strictest experiments for decades. Even though the Higgs boson discovery by the ATLAS [1] and CMS [2] experiments has completed and confirmed its particle content and predictions, the SM can only be an effective theory, which is valid at the low energy scales, since it is problematic in stabilizing the potential and mass associated with the Higgs boson. One of its well-known problems is the gauge hierarchy problem, which arises from ultraviolet energy scale sensitivity of the Higgs boson mass [3, 4, 5, 6, 7].

In order to solve the problems within the SM many models beyond the SM (BSM) have been proposed, and supersymmetry (SUSY) is one of the forefront candidates. The minimal supersymmetric extension of the SM (MSSM) can resolve the gauge hierarchy problem by proposing new particles (superpartners) for each of those in the SM, which differ in their spin by $1/2$. In other words, each fermion has bosonic superpartners (hereafter sparticles), while each boson has fermionic ones [8]. Such a partnering cancels the convergent loop contributions to the Higgs boson mass, since the contributions from bosons and fermions have opposite signs. In addition to solving the gauge hierarchy problem, the three gauge couplings of the SM nicely unify at a scale ($M_{\text{GUT}} \approx 2 \times 10^{16}$ GeV), and hence one can build supersymmetric grand unified theories (GUTs) to investigate physics at much higher energy scales. Since the Higgs boson mass does not depend on the ultraviolet scale within the MSSM framework, such GUT models can be linked to the low energy scale through the renormalization group equations (RGEs), which make possible to explore their implications at the current experiments.

Especially, the Higgs boson measurements provide a strong hint for the BSM physics. Even though it is possible to fit the current measurements within the MSSM framework, they severely constrain the fundamental parameter space of the SUSY models. The tree-level mass of the Higgs boson cannot be greater than the Z-boson mass (M_Z), and hence it needs to be corrected with the loop corrections. This fact is very effective in shaping the fundamental parameter space of MSSM. Since the Yukawa couplings of the first two families are negligible, the third family matter sparticles are the only sources to yield large radiative corrections. Moreover, the contributions from sbottom and stau, sparticles of bottom quark and tau lepton respectively, are proportional to their mixing $\mu \tan \beta$. These sparticles can easily destabilize the Higgs potential [9], the bound on these sparticles allow only minor contributions to the Higgs boson mass. On the other hand, mixing of the stop, sparticle of top quark, is inversely proportional to $\tan \beta$; thus, it has more freedom without disturbing the Higgs potential stability.

As a result, the stop sector forms the main source of the large radiative corrections with which the Higgs boson mass can be found consistent with the current experimental results. The effect of the Higgs mass constraint on the stop sector can be analyzed depending on the stop mixing. If the mixing is small (i.e. $m_{\tilde{t}_L} \approx m_{\tilde{t}_R}$), the solutions with $m_{\tilde{t}} \lesssim 800$ GeV are excluded. If one sets a large mixing between left and right-handed stops, then one can realize much lighter stop solutions, while the second stop should be heavier than 1 TeV [10]. In addition, the stop sector can be constrained by the null results from the direct searches of the sparticles at the Large Hadron Collider (LHC). The mass bound on the stop from these experiments depends on the possible decays channels. If stop is kinematically allowed only to decay into a charm quark and neutralino, then the stop mass bound can

be as low as about 230 GeV [11]. The constraint becomes much severer when the stop can decay into a bottom quark, a W – boson and a neutralino. In this case the solutions with stop mass lighter than 650 GeV are excluded [12]. The most strict channel is the one in which the stop decays into a top quark and a neutralino. This channel bounds the stop mass from below at about 750 GeV [13].

In order to solve the gauge hierarchy problem in a natural way, the stop and top quarks needs to have comparable masses, even after the SUSY breaking. However, the constraints mentioned above yield a sizeable mass splitting between the stop and top quarks. It is still possible to avoid the gauge hierarchy problem with the contribution from the trilinear terms between the stops and the Higgs boson, which is proportional to A –term in the soft supersymmetry breaking (SSB) Lagrangian. Even though the experimental constraints can be satisfied in MSSM, they yield a heavy mass spectrum for the sparticles, which brings us back to the naturalness problem. The natural region in SUSY models is characterized with $m_{\tilde{t}_1}, m_{\tilde{t}_2}, m_{\tilde{b}_1} \lesssim 500$ GeV, where $m_{\tilde{t}_{1,2}}$ are the lightest and the heaviest mass eigenstates of the stop quarks respectively, and similarly $m_{\tilde{b}_1}$ is the lightest sbottom quark. Clearly, it is not possible to fit all these sparticles in the natural region, but the required fine-tuning, which determines the deviation from the natural region, can be quantified with a parameter Δ_{EW} . In this paper, we consider the MSSM framework with non-universal gauginos ($M_1 \neq M_2 \neq M_3$) and explore the regions with acceptable fine-tuning. After the physical implications of such regions are investigated, we focus on the solutions with the stop mass lighter than 700 GeV, and discuss the LHC exclusion for these light stop solutions over some benchmark points.

The outline of our paper is the following: We first define the parameter to determine the required fine-tuning at the low scale in section 2. We also discuss the implications and restrictions from the fine-tuning constraint in this section. Section 3 describes the data generation and analyses along with the fundamental parameter space and the experimental constraints employed in our analyzes. Then, we discuss our results for the fine-tuning with highlighting the light stop solutions ($m_{\tilde{t}_1} \lesssim 700$ GeV) in Section 4. After discussing the impact of the fine-tuning and light stop solutions, we also present the mass spectrum for the other sparticles in Section 5. In Section 6 we analyze if the LHC can detect such light stop solutions over some benchmark points. Finally we conclude in Section 7.

2 Low Scale Fine-Tuning Measurement

After the Higgs boson discovery, the electroweak symmetry (EW) breaking and its nature has been understood more precise. Even though the predictions are very accurate, the EW breaking is relied on an assumption within the SM that the squared-mass parameter should be negative ($\mu^2 < 0$). Confronting with the precision data from the experiments the EW breaking scale is determined at about 100 GeV. In this case, one can ask how the divergent contributions to the Higgs boson mass yields such a finite EW scale, and what a source can yield $\mu^2 < 0$. The Higgs sector is more complicated in MSSM, since it has two Higgs doublets (H_d and H_u) in its scalar potential. Even though there is no EW breaking at some high scales, the loop corrections can trigger the EW breaking, and it can happen at a scale during the RGE runs. Including the SSB mass terms for these Higgs doublets (m_{H_d}, m_{H_u}), the EW breaking scale can be determined with the parameters; $\mu^2, m_{H_u}^2, m_{H_d}^2$ along with $\tan \beta$, where $\tan \beta$ is the ratio of vacuum expectation values (VEVs) of the MSSM Higgs

doublets. The EW breaking scale can be determined with the Z -boson mass, which can be written as [8]

$$\frac{1}{2}M_Z^2 = -\mu^2 + \frac{(m_{H_d}^2 + \Sigma_d) - (m_{H_u}^2 + \Sigma_u) \tan^2 \beta}{\tan^2 \beta - 1}, \quad (1)$$

where $\Sigma_{d,u}$ denote the radiative effects from the Higgs potential. The left hand side of Eq.(1) is determined precisely by the experiments, while the right hand side is involved with the fundamental parameters of the model. These fundamental parameters can lie in a wide range, and hence, there should be significant cancellations among them in order to realize the correct scale for the EW breaking ($M_Z = 91.2$ GeV) when they are large. The required fine-tuning arising from such cancellations can be quantified with a parameter, Δ_{EW} defined as

$$\Delta_{EW} \equiv \text{Max}(C_i)/(M_Z^2/2), \quad \text{where } C_i = \begin{cases} C_{H_d} = |m_{H_d}^2/(\tan^2 \beta - 1)| \\ C_{H_u} = |m_{H_u}^2 \tan^2 \beta/(\tan^2 \beta - 1)| \\ C_\mu = |-\mu^2| \end{cases} \quad (2)$$

here we assume that the masses include the radiative corrections as $m_{H_{u,d}} \equiv m_{H_{u,d}} + \Sigma_{u,d}$. In contrast to the natural region, which is characterized with the stop and sbottom masses, the fine-tuning does not depend on these masses directly. As seen from Eq.(2), C_{H_d} is suppressed by $\tan \beta$, and from moderate to large values of this parameter, the fine-tuning is determined mostly by μ and m_{H_u} , and the correct M_Z requires $\mu^2 \approx -m_{H_u}^2$.

If it is possible to realize low μ^2 values over the fundamental parameter space, the fine-tuning can be found in an acceptable range regardless to the sparticle mass spectrum. However, the effects from the sparticle masses are encoded in the radiative corrections. Σ_d is evolved with the sbottom and stau masses, which contribute to m_{H_d} at the loop level. Since this term is suppressed by $\tan \beta$, the effects from the sbottom and stau masses in the fine-tuning are minor. On the other hand, Σ_u , which arises from the stop sector, does not exhibit a suppression by $\tan \beta$. Large stop masses or large mixings between left and right handed stops can significantly contribute to the radiative corrections which result in large m_{H_u} , and thus large μ -term. Considering the severe experimental exclusion limits on stops, discussed in the previous section, it is obvious that the parameter space, allowed by the experiments, needs to be largely fine-tuned. Even if one restricts the lightest stop masses to be at a few hundred GeV, then a large mixing between stops is required by the Higgs boson mass. Such a large mixing results in very large radiative corrections, and hence, it raises the required fine-tuning significantly [14]. This discussion can be concluded that the SUSY models needs large fine-tuning when the sparticle and the gaugino masses are set universal at the GUT scale.

If one relaxes the exclusion limits from the LHC, mentioned above, and allows the solutions with light stop, the required fine-tuning can potentially be improved at the low scale. However, the requirement to yield the Higgs boson of mass about 125 GeV also puts a severe constraint on the stop masses as discussed in the previous section. The Higgs boson mass within the MSSM can be written as

$$m_h \approx M_Z \cos \beta + \frac{3m_t^4}{4\pi^2 v^2} \left(\text{Log} \frac{M_S^2}{m_t^2} + \frac{X_t}{M_S^2} - \frac{X_t^4}{12M_S^4} \right) - \frac{y_b^4 \mu^4 v^2}{16\pi^2 M_S^4} \quad (3)$$

where m_t is the top quark mass, while $M_S \equiv \sqrt{m_{\tilde{t}_L} m_{\tilde{t}_R}}$ is the average stop quark mass. M_S is also the energy scale at which the supersymmetric particles decouple from the SM. The mixing in the stop sector is encoded in X_t as $X_t = A_t - \mu \cot \beta$, where A_t stands for this mixing. The first term in Eq.(3) is the tree-level mass of the Higgs, and it can only be about 90 GeV at most. Thus, it needs significant loop corrections to realize the Higgs boson of mass about 125 GeV. Such large corrections can be obtained with a large mass splitting between the stop and top quarks ($M_S \gg m_t$). Another way to raise the loop corrections is to implement large mixing in the stop sector. We should note that here $A_t \lesssim 3M_S$ should be satisfied not to break color and/or charge conservation at minima of the scalar potential [15]. Hence, in the case of large mixing, sparticles cannot be lighter than certain mass scales.

The last term in Eq.(3) represents loop contributions from the bottom sector, but this term is relevant only for large $\tan \beta$. Consequently, the only dominant source for large loop corrections to the Higgs boson mass is the stop sector, which require stop quarks to be heavier even if the mixing in this sector is large. This situation can be drastically different if MSSM is extended with new particles and/or new symmetries [16, 17, 18, 19, 20, 21] which contribute to the Higgs boson mass as significantly as the stop quarks. In this context, the minimal supersymmetric models may not cover the full picture of physics. The mechanisms, which are not included in the minimal models, can effect the low scale phenomenology. In this sense, the fine-tuning requirement can emerge because of some missing mechanisms, and its amount can be interpreted the effectiveness of these missing mechanisms, and also indicates the amount of deviation from the minimality. The effects from missing mechanisms can be analyzed also within the MSSM framework by implementing non-universalities in gaugino and scalar sectors [22, 23, 24, 25]

In our work, we analyze the effects of possible missing mechanisms within the MSSM framework by imposing non-universality in the gaugino sector. While we focus on the regions with low fine-tuning, we also highlight the stop quark masses less than 700 GeV, and discuss if such solutions can still survive under the severe experimental constraints.

3 Scanning Procedure and Experimental Constraints

We have employed SPheno 3.3.8 package [26, 27] obtained with SARAH 4.5.8 [28, 29]. In this package, the weak scale values of the gauge and Yukawa couplings presence in MSSM are evolved to the unification scale M_{GUT} via the renormalization group equations (RGEs). M_{GUT} is determined by the requirement of the gauge coupling unification through their RGE evolutions. Note that we do not strictly enforce the unification condition $g_1 = g_2 = g_3$ at M_{GUT} since a few percent deviation from the unification can be assigned to unknown GUT-scale threshold corrections [30, 31]. With the boundary conditions given at M_{GUT} , all the SSB parameters along with the gauge and Yukawa couplings are evolved back to the weak scale.

We have performed random scans over the following parameter space

$$\begin{aligned}
0 &\leq m_0 \leq 10 \text{ TeV} \\
-10 &\leq M_1 \leq 0 \text{ TeV} \\
-10 &\leq M_2 \leq 0 \text{ TeV} \\
0 &\leq M_3 \leq 10 \text{ TeV} \\
-3 &\leq A_0/m_0 \leq 3 \\
2 &\leq \tan \beta \leq 60 \\
\mu &< 0, \quad m_t = 173.3 \text{ GeV}
\end{aligned} \tag{4}$$

where m_0 is the universal SSB mass term for the matter scalars and Higgs fields. M_3 , M_2 and M_1 are SSB mass terms for the gauginos associated with the SU(3), SU(2) and U(1) symmetry groups respectively. A_0 is SSB trilinear coupling, and $\tan \beta$ is ratio of VEVs of the MSSM Higgs doublets. In the constrained MSSM (CMSSM) with non-universal gauginos all matter scalars have the same mass and gaugino masses can be chosen different each other at the GUT scale. The radiative EW breaking (REWSB) condition determines the value of μ - term but not its sign; thus, its sign is one of the free parameters, and we set it negative in our scans. In addition, we have used central value of top quark mass as $m_t = 173.3$ GeV [32]. Note that the sparticle spectrum is not too sensitive in one or two sigma variation in the top quark mass [33], but it can shift the Higgs boson mass by 1-2 GeV [34, 35].

The REWSB condition provides a strict theoretical constraint [36, 37, 38, 39, 40] over the fundamental parameter space given in Eq.(4). Another important constraint comes from the relic abundance of charged supersymmetric particles. This constraint excludes the regions which yield charged particles such as stop and stau being the lightest supersymmetric particle (LSP) [41]. In this context, we accept only the solutions which satisfy the REWSB condition and yield neutralino LSP.

In scanning the parameter space we use our interface, which employs Metropolis-Hasting algorithm described in [42, 43]. After collecting the data, we successively apply the mass bounds on all sparticles [44] and the constraints from the rare B-decays ($B_s \rightarrow \mu^+ \mu^-$ [45], $B_s \rightarrow X_s \gamma$ [46] and $B_u \rightarrow \tau \nu_\tau$ [47]). The experimental constraints can be listed as follows:

$$\begin{aligned}
123 &\leq m_h \leq 127 \text{ GeV} \\
m_{\tilde{g}} &\geq 1000 \text{ GeV} \\
0.8 \times 10^{-9} &\leq BR(B_s \rightarrow \mu^+ \mu^-) \leq 6.2 \times 10^{-9} \quad (2\sigma) \\
2.9 \times 10^{-4} &\leq BR(b \rightarrow s \gamma) \leq 3.87 \times 10^{-4} \quad (2\sigma) \\
0.15 &\leq \frac{BR(B_u \rightarrow \nu_\tau \tau)_{MSSM}}{BR(B_u \rightarrow \nu_\tau \tau)_{SM}} \leq 2.41 \quad (3\sigma)
\end{aligned} \tag{5}$$

We have imposed these bounds on the Higgs boson [1, 2] and the gluino [48], since they have updated by the current experiments. One of the strongest constraint is come from rare B-meson decay into a muon pair. The supersymmetric contribution to the

$BR(B_s \rightarrow \mu^+ \mu^-)$ is severely constrained, since the SM's predictions almost overlap with its experimental measurements. Supersymmetric contribution to this process is proportional to $(\tan \beta)^6 / m_A^4$. Therefore, it has a strong impact on the regions with large $\tan \beta$ that CP-odd Higgs boson has to be heavy enough ($m_A \sim \text{TeV}$) to suppress the supersymmetric contribution.

4 Fine-Tuning and Sparticle Mass Spectrum in MSSM

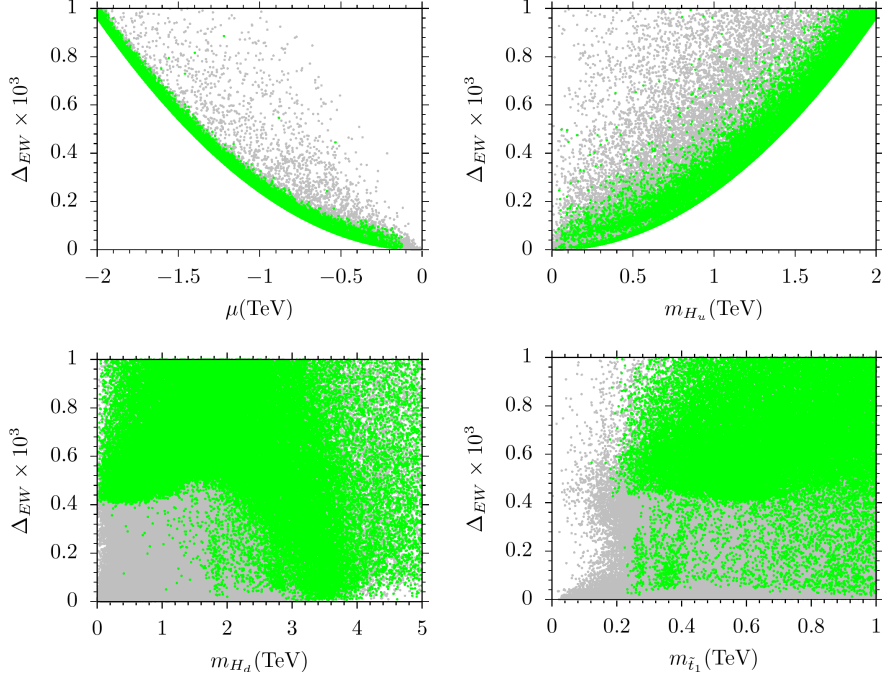


Figure 1: Plots in $\Delta_{EW} - \mu$, $\Delta_{EW} - m_{H_u}$, $\Delta_{EW} - m_{H_d}$, and $\Delta_{EW} - m_{\tilde{t}_1}$ planes. All points are consistent with REWSB and neutralino LSP. Gray points are excluded by the current experimental bounds, while the green points are allowed.

We present our results about the fine-tuning and the stop masses in this section. We highlight the fine-tuning and stop mass correlation. The acceptable fine-tuning amount can be determined in terms of Δ_{EW} by conventionally applying the condition $\Delta_{EW} \leq 10^3$. Figure 1 represents our results with plots in $\Delta_{EW} - \mu$, $\Delta_{EW} - m_{H_u}$, $\Delta_{EW} - m_{H_d}$, and $\Delta_{EW} - m_{\tilde{t}_1}$ planes. All points are consistent with REWSB and neutralino LSP. Gray points are excluded by the current experimental bounds, while the green points are allowed. The $\Delta_{EW} - \mu$ plane reveals the strong dependence of Δ_{EW} on the μ -term. If one seeks to stay in the acceptable fine-tuning region with $\Delta_{EW} \leq 10^3$, the μ -term can be only as high as -2 TeV. Beyond this value, the fine-tuning condition cannot be satisfied. The correlation between the fine-tuning and μ -term is represented in a tight parabolic curve obtained from our data, and this curve is compatible with the discussion of Section 2 that the μ -term is the most effective parameter in determining the fine-tuning amount. A similar curve can be seen in the $\Delta_{EW} - m_{H_u}$ plane, even though it is not as tight as in the correlation with the μ -term. This results also reflects the impact of the condition $\mu \approx m_{H_u}$ in order to realize the correct EW breaking scale according to Eq.(2) ($M_Z \sim 90$ GeV). The $\Delta_{EW} - m_{H_d}$ plane

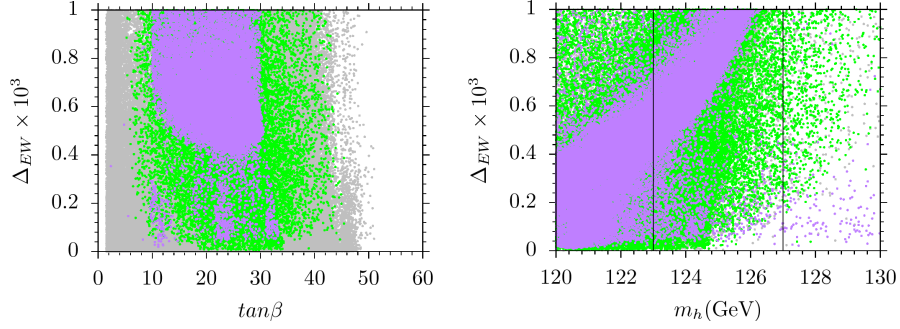


Figure 2: Plots in $\Delta_{EW} - \tan \beta$ and $\Delta_{EW} - m_h$ planes. The color coding is the same as Figure 1. In addition, the purple points form a subset of green and they represent the solutions with $m_{\tilde{t}_1} \leq 700$ GeV. We do not apply the Higgs mass bound in the $\Delta_{EW} - m_h$ plane, since it is represented in one axis. We use rather vertical lines which shows the experimental bounds on the Higgs boson mass.

shows that it is possible to realize low fine-tuning for any value of m_{H_d} . Recall that the contribution to the fine-tuning from m_{H_d} is suppressed by $\tan \beta$, so that the fine-tuning is mostly determined with the interplay between the μ -term and m_{H_u} . The last panel in Figure 1 displays the stop mass and fine-tuning in the $\Delta_{EW} - m_{\tilde{t}}$ plane. According to our results, the stop mass can be as light as about 200 GeV. As seen from this plane, there are plenty of solutions (green) which yield light stops and acceptable fine-tuning at the low scale. In this plane, we apply only the constraints listed in Eq.(5) including the Higgs mass, while the collider constraints, which are based on the decay channels of stops, are not applied yet. The light stop solutions can be restricted further with these constraints, which are analyzed later separately.

Figure 2 displays the results with plots in $\Delta_{EW} - \tan \beta$ and $\Delta_{EW} - m_h$ planes. The color coding is the same as Figure 1. In addition, the purple points form a subset of green and they represent the solutions with $m_{\tilde{t}_1} \leq 700$ GeV. We do not apply the Higgs mass bound in the $\Delta_{EW} - m_h$ plane, since it is represented in one axis. We use rather vertical lines which shows the experimental bounds on the Higgs boson mass. The $\Delta_{EW} - \tan \beta$ plane exhibits a restriction in $\tan \beta$ range that this parameter cannot take a value greater than 50. On the other hand, this restriction on this parameter does not arise from the fine-tuning condition, it is rather related to the REWSB condition. In the allowed range it is possible to obtain low fine-tuning for any value of $\tan \beta$. If one applies another condition on the stop mass such that $m_{\tilde{t}_1} \leq 700$ GeV, the solutions restrict the parameter space as $10 \lesssim \tan \beta \lesssim 30$ (purple). We also present the correlation between the fine-tuning and the Higgs boson mass in the $\Delta_{EW} - m_h$. The results reflect the fact that if the Higgs boson was found much lighter than its current experimental range, the minimal SUSY models could not suffer from large fine-tuning issues. The $\Delta_{EW} - m_h$ plane shows that Δ_{EW} can be as low as about zero, which means no fine-tuning is required, when the Higgs boson mass is about 120 GeV. However these regions have been already excluded. The experimental results allow only the region between two vertical lines in the plane. One can easily see that the fine-tuning can go worse as the Higgs boson mass increases.

In addition, there is another branch seen from the $\Delta_{EW} - m_h$ plane in which Δ_{EW} remains almost constant ($\Delta_{EW} \sim 100 - 200$), despite the increase in the Higgs boson mass. The solutions in this branch can be understood with the effect from the mixing of the left

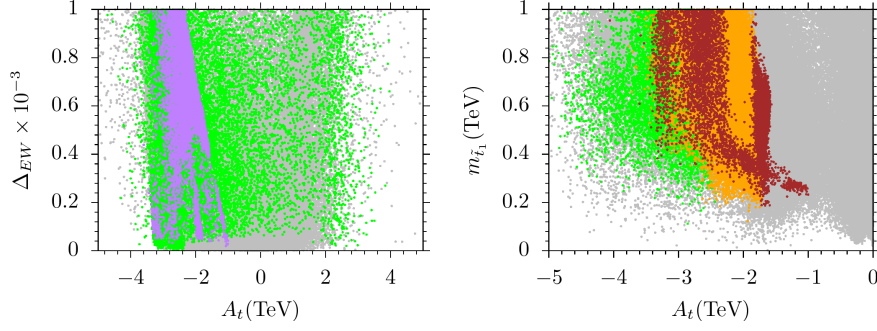


Figure 3: Plots in $\Delta_{EW} - A_t$ and $m_{\tilde{t}_1} - A_t$ planes. The color coding in the left panel is the same as Figure 1. While the meaning of gray and green are the same in the right panel, the orange points represents the solutions with $\Delta_{EW} \leq 10^3$, and the brown points form a subset of orange with $\Delta_{EW} \leq 500$. The condition $m_{\tilde{t}_1} \leq 700$ GeV is not applied in the right panel, since the stop mass is represented directly in one axis.

and right-handed stops, which is proportional to A_t . We discuss this effect with plots in $\Delta_{EW} - A_t$ and $m_{\tilde{t}_1} - A_t$ planes of Figure 3. The color coding in the left panel is the same as Figure 1. While the meaning of gray and green are the same in the right panel, the orange points represents the solutions with $\Delta_{EW} \leq 10^3$, and the brown points form a subset of orange with $\Delta_{EW} \leq 500$. The condition $m_{\tilde{t}_1} \leq 700$ GeV is not applied in the right panel, since the stop mass is represented directly in one axis. The $\Delta_{EW} - A_t$ plane shows that the solutions with acceptable fine-tuning (shown in purple) require A_t from about 1 to 4 TeV in the negative region. The negative sign of A_t reverses the effect of stop mixings in the fine-tuning calculations. In this context, the positive values of A_t , even in the range 1 – 4 TeV cause high fine-tuned solutions, and hence one cannot find any purple point in the positive A_t region. The branch with constant Δ_{EW} mentioned above can also be seen in the $m_{\tilde{t}_1} - A_t$ plane. In one branch, A_t and the stop mass change together and they yield an increase in the fine-tuning as well. In the second branch, A_t remains constant at about -1.8 TeV, while the stop mass increases up to about a TeV. The constant A_t and fine-tuning and increasing the stop mass in this branch can be concluded that stop mass is not a strong parameter in the fine-tuning, in contrast to expected, while A_t is determining the behavior of the solutions in respect of the fine-tuning.

5 Sparticle Mass Spectrum

We discussed the fine-tuning impact over the parameter space and light stop solutions in the previous section. Even though they are not as dominant as the stop in the fine-tuning and the Higgs boson mass, the other sparticles are also of importance in exploring the low scale implications. This section will represent our results for the other sparticle masses such as the heaviest stop ($m_{\tilde{t}_2}$), ($m_{\tilde{g}}$), the lightest sbottom ($m_{\tilde{b}_1}$), and the lightest stau ($m_{\tilde{\tau}_1}$) in Figure 4 with plots in $m_{\tilde{t}_1} - m_{\tilde{t}_2}$, $m_{\tilde{t}_1} - m_{\tilde{g}}$, $m_{\tilde{t}_1} - m_{\tilde{b}_1}$, and $m_{\tilde{t}_1} - m_{\tilde{\tau}_1}$. The color coding is the same as the right panel of Figure 3. The $m_{\tilde{t}_1} - m_{\tilde{t}_2}$ plane shows that the heaviest stop quark cannot be lighter than about 1 TeV, even if the lightest stop mass is can be found as light as about 200 GeV. This mass difference between the two stop quarks is a result of a large mixing in the stop sector. If the lightest stop mass is about a few

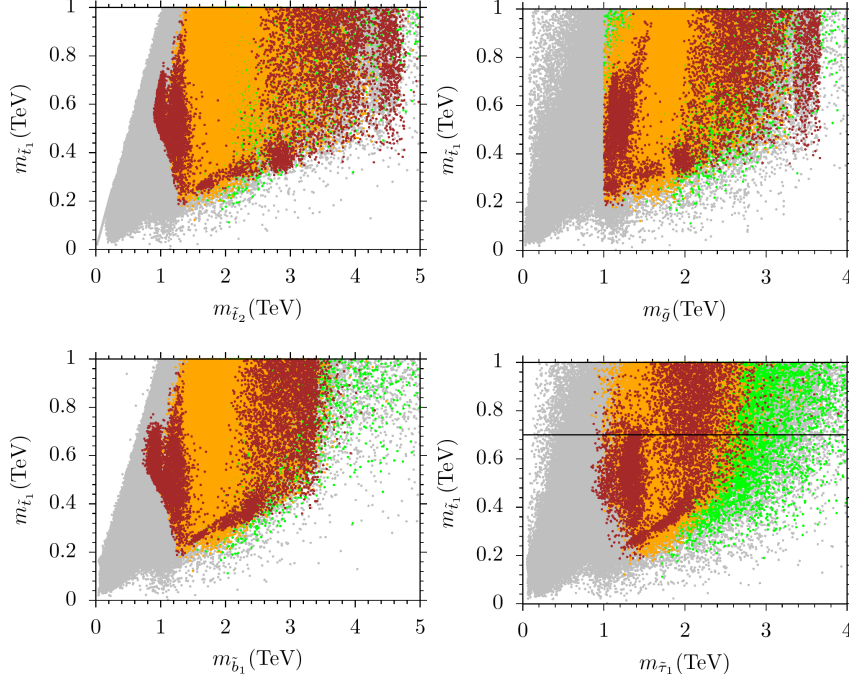


Figure 4: The sparticle masses in $m_{\tilde{t}_1} - m_{\tilde{t}_2}$, $m_{\tilde{t}_1} - m_{\tilde{g}}$, $m_{\tilde{t}_1} - m_{\tilde{b}_1}$, and $m_{\tilde{t}_1} - m_{\tilde{\tau}_1}$. The color coding is the same as the right panel of Figure 3.

hundred GeV, the Higgs boson mass should be fed with the second stop and mixing in the stop sector to be consistent with the experimental results. In this context, the condition on the stop mass lighter than 700 GeV pushes the heavier stop mass to the TeV scale and above. This can happen only if the mixing between two stops are large as shown in the previous section. Another sparticle effective in the stop mass is the gluino. Even though the stop mass seems to be determined with the universal scalar mass at the GUT scale, the gluino contributes to the stop mass at loop levels. As seen from the $m_{\tilde{t}_1} - m_{\tilde{g}}$, a linear correlation can be realized between the lightest stop and gluino masses. The lightest stop mass can be as low as 200 GeV for $m_{\tilde{g}} \sim 1\text{TeV}$, while $m_{\tilde{t}_1} \gtrsim 400\text{ GeV}$, when $m_{\tilde{g}} \gtrsim 3\text{ TeV}$. We can have light stop solutions even the gluino mass is at about a few TeV scale, because of the non-universality in the gaugino masses as given in Eq.(4). If one sets the gaugino masses universal at the GUT scale, it is not possible to obtain the stop masses below a TeV, when gluino has a mass about a few TeV [14].

Another sparticle, whose mass defines the natural region, is sbottom. As mentioned before, the natural region is characterized with $m_{\tilde{b}_1} \lesssim 500\text{ GeV}$ along with the stop masses. The $m_{\tilde{t}_1} - m_{\tilde{b}_1}$ plane shows that sbottom should be heavier than about 1 TeV when the stop has a mass about 200 GeV. On the other hand, if we consider the solutions with a stop mass about 600 GeV, then it is possible to find solutions with $m_{\tilde{b}_1} \approx 600\text{ GeV}$, which yields an approximate degeneracy in mass between the lightest stop and sbottom. In this degeneracy region their masses are very close to the characteristics of the natural region. However, since the heaviest stop mass is more than 1 TeV, such solutions still deviate from the natural region, and they need to be fine-tuned proportionally to the heaviest stop mass and stop mixing. Finally, we present the spectrum in the leptonic sector in stau mass. As seen from the $m_{\tilde{t}_1} - m_{\tilde{\tau}_1}$ plane, the stau cannot be lighter than about 800 GeV. Since the stau is the lightest slepton, other sleptons from the first two families (smuon and selectron)

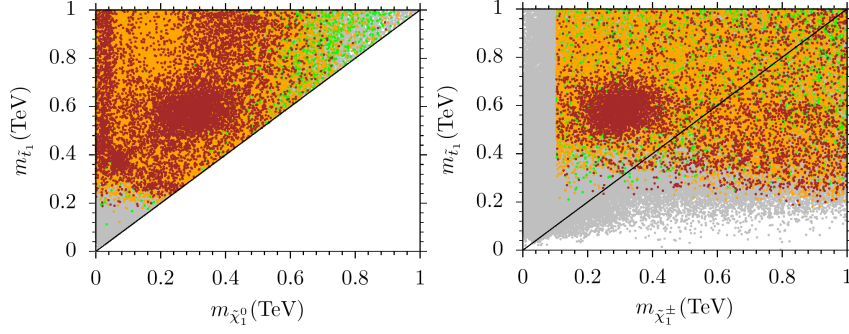


Figure 5: Plots in $m_{\tilde{t}_1} - m_{\tilde{\chi}_1^0}$, $m_{\tilde{t}_1} - m_{\tilde{\chi}_1^\pm}$ planes. The color coding is the same as the right panel of Figure 3. The diagonal line indicates the mass degeneracy between the plotted particles.

are expected to be much heavier than stau.

Before concluding this section, we also consider the masses of neutralino and chargino. Since we require the solutions to be compatible with neutralino LSP, neutralino has to be included in final states in decay channels of supersymmetric particles. Besides, neutralino and chargino take part in main decay channels of stop, which are of importance in possible signal analyses and stop detection at LHC. Since the signal analyses also depend on masses of these particles, we present our results in Figure 5 with plots in $m_{\tilde{t}_1} - m_{\tilde{\chi}_1^0}$, $m_{\tilde{t}_1} - m_{\tilde{\chi}_1^\pm}$ planes. The color coding is the same as the right panel of Figure 3. The diagonal line indicates the mass degeneracy between the plotted particles. The $m_{\tilde{t}_1} - m_{\tilde{\chi}_1^0}$ plane shows that the neutralino can be found almost massless even after the experimental constraints are applied. Following the diagonal line in this plane, it is also possible to find plenty of solutions in which neutralino and stop are degenerate in mass. Similarly, according to the $m_{\tilde{t}_1} - m_{\tilde{\chi}_1^\pm}$ plane, chargino can be as light as about 100 GeV. The solutions with chargino lighter than 100 GeV are also excluded by the LEP II results [44].

6 LHC Escape of Light Stops

We have discussed the fine-tuning and sparticle mass spectrum with a special emphasize on the stop mass in previous sections. As mentioned earlier, the current mass bounds on the stop quarks are very severe depending on the decay channels of stop. The severest bound comes from the process $\tilde{t}_1 \rightarrow t\tilde{\chi}_1^0$, which excludes the solutions with $m_{\tilde{t}_1} \lesssim 700$ GeV. Another decay channel of stop in which stop decays into a bottom quark, a W -boson and a neutralino also brings a severe bound and it excludes the solutions with $m_{\tilde{t}_1} \lesssim 650$ GeV. Stop can also decay into a charm quark and a neutralino, but analyses from this channel excludes only if stop quarks are lighter than about 230 GeV. These three channels are the main cascades of stop quark in signal analyses and possible detection mechanisms of stop at LHC.

In this section we will consider possible decay cascades of the stop quark, and discuss the detection probability by comparing with the relevant background process, which is constructed within the (non-supersymmetric) SM framework. The signal cascades and background can be listed as follows;

Table 1: Benchmark points related to the Signal – a are presented. The background cross-section for Signal – a is 22.71 pb. All masses are given in GeV.

$m_{\tilde{t}_1}$	$m_{\tilde{\chi}_1^\pm}$	$m_{\tilde{\chi}_1^0}$	$BR(\tilde{t}_1 \rightarrow \tilde{\chi}_1^0 t)$	$BR(\tilde{t}_1 \rightarrow \tilde{\chi}_1^\pm b)$	$BR(\tilde{\chi}_1^\pm \rightarrow \tilde{\chi}_1^0 W^\pm)$	$\sigma(pb)$	Δ_{EW}
203.06	909.44	19.86	1	–	0.75	1.388	447.86
359.12	681.20	72.21	1	–	0.03	7.68×10^{-2}	446.02
428.60	210.57	62.68	0.83	0.14	1	2.02×10^{-2}	452.52
505.75	213.66	84.47	0.85	0.11	1	8.46×10^{-3}	441.83
616.95	184.13	83.48	0.73	0.19	1	1.89×10^{-3}	457.28
697.29	146.47	146.28	0.30	0.69	–	1.63×10^{-4}	439.98

Table 2: Benchmark points related to the Signal – b are presented. The background cross-section for Signal – b is 22.71 pb. All masses are given in GeV.

$m_{\tilde{t}_1}$	$m_{\tilde{\chi}_1^\pm}$	$m_{\tilde{\chi}_1^0}$	$BR(\tilde{t}_1 \rightarrow \tilde{\chi}_1^0 t)$	$BR(\tilde{t}_1 \rightarrow \tilde{\chi}_1^\pm b)$	$BR(\tilde{\chi}_1^\pm \rightarrow \tilde{\chi}_1^0 W^\pm)$	$\sigma(pb)$	Δ_{EW}
462.26	173.57	34.58	0.67	0.25	1	1.46×10^{-3}	424.13
505.75	213.66	84.47	0.85	0.11	1	1.74×10^{-4}	441.83
616.95	184.13	83.48	0.73	0.19	1	1.71×10^{-4}	457.28
676.39	376.39	269.64	0.77	0.17	1	7.8×10^{-5}	444.87

$$\text{Signal – a)} \quad pp \rightarrow \tilde{t}\tilde{t}^* \rightarrow t\bar{t}\tilde{\chi}_1^0\tilde{\chi}_1^0 \rightarrow b\bar{b}W^\pm W^{\pm*}\tilde{\chi}_1^0\tilde{\chi}_1^0 \rightarrow b\bar{b}l^\pm\bar{l}^\pm\nu_l\bar{\nu}_l\tilde{\chi}_1^0\tilde{\chi}_1^0$$

$$\text{Signal – b)} \quad pp \rightarrow \tilde{t}\tilde{t}^* \rightarrow b\bar{b}\tilde{\chi}_1^\pm\tilde{\chi}_1^\pm \rightarrow b\bar{b}W^\pm W^{\pm*}\tilde{\chi}_1^0\tilde{\chi}_1^0 \rightarrow b\bar{b}l^\pm\bar{l}^\pm\nu_l\bar{\nu}_l\tilde{\chi}_1^0\tilde{\chi}_1^0 \quad (6)$$

$$\text{SM background :} \quad pp \rightarrow t\bar{t} \rightarrow b\bar{b}W^\pm W^{\pm*} \rightarrow b\bar{b}l^\pm\bar{l}^\pm\nu_l\bar{\nu}_l$$

Even though the signal processes yield the same final states, they differ in the cascades. Signal – a evolves with a process in which a stop pair decays into top quarks and neutralinos, while, in Signal – b, $\tilde{t} \rightarrow b\tilde{\chi}^\pm$ takes place. These two signals can be distinguished from each other in a way depending on neutralino and chargino masses. Signal – a can be allowed kinematically only when $m_{\tilde{t}} - m_{\tilde{\chi}^0} \gtrsim m_t$. Otherwise, Signal – b is the dominant channel in analyses with the condition that $m_{\tilde{t}} - m_{\tilde{\chi}^\pm} \gtrsim m_b$, where $m_b \approx 4$ GeV. If these two conditions are satisfied, neither of the channels listed in Eq.(6) are allowed. In such cases, stop usually decays into a charm quark and a neutralino, which provides a very soft signal and the exclusion limit on the stop mass is not very strict, and hence it is not considered in our work. The relevant background process is also given in Eq.(6), and it is the same for both signal processes.

A possible detection at the colliders require that the signal process should suppress the background and give more events (at least 5 events more). In Figure 6 we represent the comparison of the signal processes with the background. Top panels represent the event numbers in comparison with the background for Signal – a, while the bottom panels are for Signal – b. The legend is given in side of each plot. Each signal is analyzed for different benchmark points given in Tables 1 and 2. The benchmark points are chosen with the requirements that they have to be consistent with the constraints given in Eq.(5), and yield a low fine-tuning amount ($\Delta_{EW} \leq 500$). We also require the benchmark points to give the highest cross-section for the signals under concern. We especially focus on the light mass scales for the stop quark, which are claimed to be excluded by LHC. As is seen from the plots in Figure 6, there is no benchmark point, which can suppress the background and

reach to the detectable region. The cross-section for the background process is about 22.71 pb, while the highest cross-section, obtained from Signal – a with $m_{\tilde{t}} \approx 203$ GeV, is found as about 1.39 pb, which is one magnitude order smaller than the background. The similar discussion can follow for Signal – b represented with the bottom panels in Figure 6. There is no solutions found which can suppress the background. The highest cross-section for Signal – b process is obtained for a solution with $m_{\tilde{t}} \approx 460$ GeV, and it is five magnitude of order smaller ($\sim 10^{-3}$) than the background. As a conclusion, our results show that, when one restricts the supersymmetric models from the GUT scale, the solutions can escape from detection at the LHC experiments, even if the stop masses are found in the excluded region. Note that the signal cross-sections can be enhanced in low scale analyses without considering the GUT scale origin, since supersymmetric models have lots of free parameter at the low scale. However, this freedom is restricted significantly in supersymmetric GUT models, and our results show that the solutions can escape from detection, and the LHC constraints can be relaxed significantly.

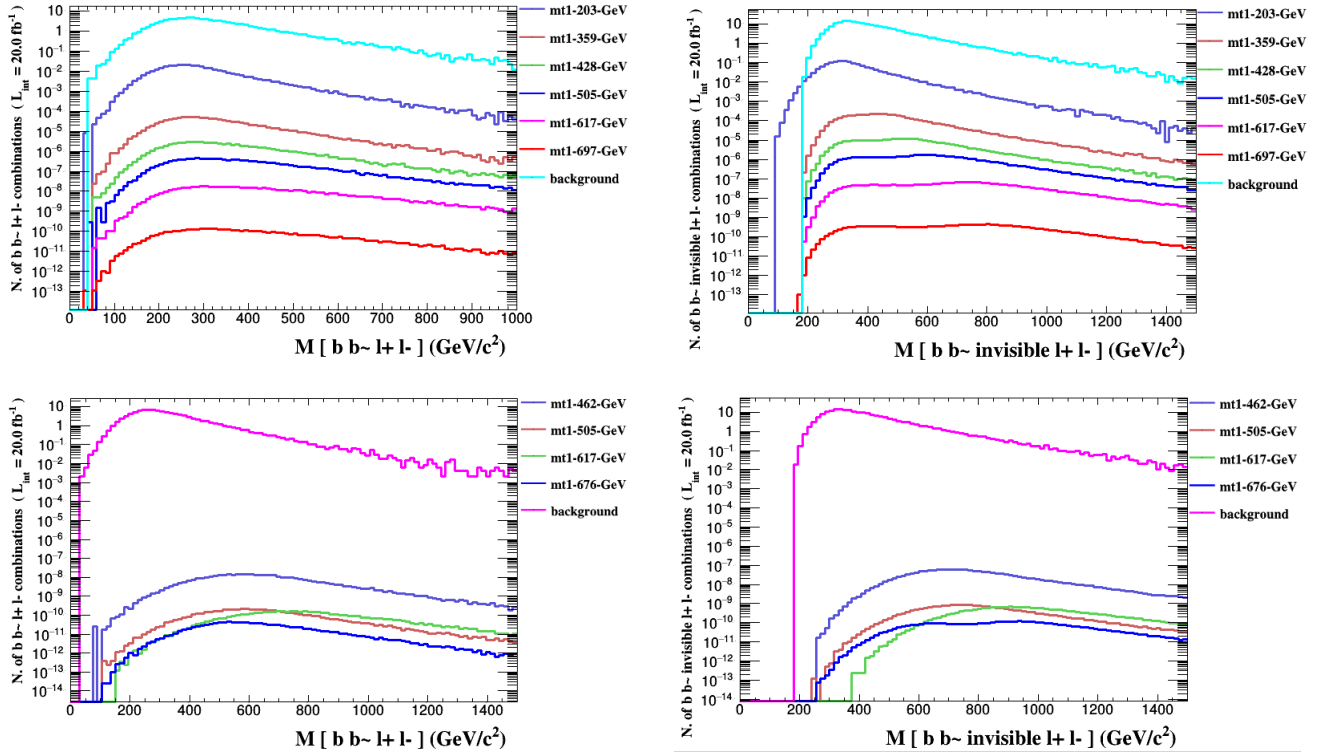


Figure 6: Plots for Event Numbers in correlation with the invariant masses of the final state particles. Top panels represent the event numbers in comparison with the background for Signal – a, while the bottom panels are for Signal – b. The legend is given in side of each plot.

These small cross-sections (and much less event numbers) can be understood by considering the stop pair production at the LHC experiments. Even though the signals are different in their decay cascades, both include stop pair production in their first chain. The relevant background for stop pair production is the top pair production whose cross-section is [49]

$$\sigma_{t\bar{t}} = [829 \pm 50(\text{stat}) \pm 56(\text{syst}) \pm 83(\text{lumi})] \text{ pb}. \quad (7)$$

While the top pair production has a large cross-section, the stop pair production yields much smaller cross-section as shown in Figure 7. The cross-section for a signal process is inversely proportional to the masses of the relevant sparticles, and hence, one can naturally expect that the stop pair production can have a large cross-section when the stop quark is light. In our case, the lightest stop solution has $m_{\tilde{t}} \sim 200$ GeV. Even though this benchmark point has the largest cross-section, it is only as large as 39.37 pb, which is smaller even than the errors in cross-section measurements of top pair production given in Eq.(7).

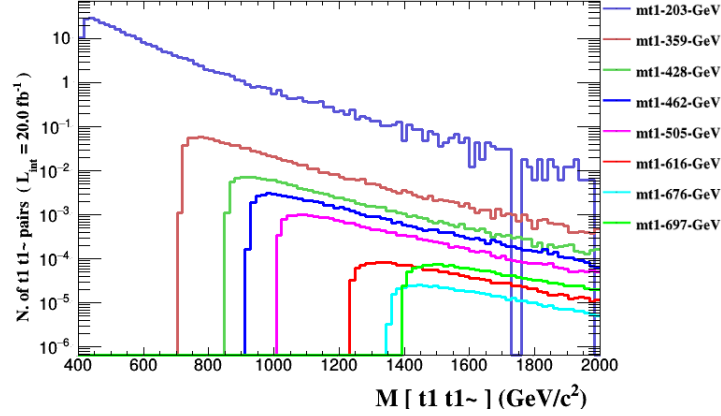


Figure 7: Stop pair production for the benchmark points in Tables 1 and 2.

7 Conclusion

We discussed the fine-tuning issue within the MSSM framework. We interpreted the fine-tuning as an indication for missing mechanisms, which can be left out in the minimal supersymmetric models. Following this idea we imposed non-universal gaugino masses at the GUT scale. We showed that the μ -term is the main parameter which determines the required fine-tuning amount, and it is possible to realize $\mu \approx 0$ consistently with the EW breaking. Even though μ is the main parameter, it also has an impact on the SSB Higgs field mass, m_{H_u} , since $\mu \approx m_{H_u}$ is required to have the EW breaking at the correct scale ($M_Z \sim 90$ GeV). On the other hand, m_{H_d} has almost no impact on the fine-tuning measurements, since its contributions are suppressed by $\tan \beta$. Any value of $\tan \beta$ can yield an acceptable amount of fine-tuning, but it is restricted to the range 10-30, if one also requires the solutions to yield light stop quarks ($m_{\tilde{t}} \leq 700$ GeV).

As is well-known, the fine-tuning requirement is closely related to the observed Higgs boson mass, and we found that the heavier Higgs boson mass solutions need to be fine-tuned more. We also realize a second branch in which the fine-tuning amount remains almost constant. In this branch A_t also remains constant, but the stop mass increases. We conclude this result that the fine-tuning is strongly correlated with the mixing (A_t) of left and right-handed stop quarks, while their masses are not effective as much as their mixing. However, a large mixing requires rather heavy stops in order to preserve the color and charge symmetry at minima of the scalar potential. While the lightest stop can be as light as 200 GeV, the heavier stop quark cannot be lighter than a TeV. This mass difference between two stops are caused by the Higgs boson mass constraint. In addition, we found

the sbottom quarks can be as light as about 600 GeV, and they can be nearly degenerate with the stop quarks in mass. Gluino mass can lie in a range 1-4 TeV, but heavy gluinos yield heavy stops since they significantly contribute to the stop mass at the loop level. Also the sparticles in the leptonic sector cannot be lighter than 1 TeV.

Finally we focused on light stop mass solutions, and discussed if LHC could detect such light stops. We found that in the best case, the possible signals has at least one magnitude order smaller than the relevant background processes. These small cross-sections cause a strong suppression over the signal by the background processes. This suppression can be understood with the stop pair production at the LHC. The relevant background for this production process is top pair production, whose cross-section is about 800 pb. We found that even lightest stop solutions can only provide about 30 pb production cross-section for a pair of stop quarks. This cross-section is much smaller than that of top quark pair production. Nevertheless, it is even smaller than errors arising in measurements of top quark pair production.

Acknowledgments

We would like to thank Qaisar Shafi, Durmuş Ali Demir, Zafer Altın, and Büşra Niş for fruitful discussions. Part of the numerical calculations reported in this paper were performed at the National Academic Network and Information Center (ULAKBİM) of The Scientific and Technological Research Council of Turkey (TUBİTAK), High Performance and Grid Computing Center (Truba Resources).

References

- [1] Aad, G.; *et al.* [ATLAS Collaboration], *Phys. Lett. B* **2012**, *716*, 1-29.
- [2] Chatrchyan, S.; *et al.* [CMS Collaboration], *JHEP* **2013**, *1306*, 081.
- [3] Gildener, E. *Phys. Rev. D* **1976**, *14*, 1667-1672.
- [4] Gildener, E. *Phys. Lett. B* **1980**, *92*, 111-114. doi:10.1016/0370-2693(80)90316-0
- [5] Weinberg, S. *Phys. Lett. B* **1979**, *82* 387-391.
- [6] Susskind, L. *Phys. Rev. D* **1979**, *20*, 2619-2625.
- [7] Veltman, M. J. G. *Acta Phys. Polon. B* **1981**, *12*, 437-457.
- [8] Martin, S. P. *Adv. Ser. Direct. High Energy Phys.* **2010**, *21*, 1-98, and references therein.
- [9] Carena, M.; Gori, S.; Low I.; Shah, N. R.; and Wagner, C. E. M *JHEP* **2013**, *1302*, 114.
- [10] Carena, M.; Gori, S.; Low I.; Shah, N. R.; and Wagner, C. E. M *JHEP* **2012**, *1203*, 014.
- [11] The ATLAS collaboration, *ATLAS-CONF-2013-068*.
- [12] Outschoorn, V. I. M. [CMS Collaboration] *EPJ Web Conf.* **2013**, *60*, 18003.

- [13] Lari, T. [ATLAS Collaboration] *PoS EPS-HEP* **2013**, 294.
- [14] Demir, D. A.; n, C. S. *Phys. Rev. D* **2014**, *90*, 095015.
- [15] U. Ellwanger and C. Hugonie, *Phys. Lett. B* **457**, 299 (1999) doi:10.1016/S0370-2693(99)00546-8 [hep-ph/9902401].
- [16] I. Gogoladze, B. He and Q. Shafi, *Phys. Lett. B* **718**, 1008 (2013) doi:10.1016/j.physletb.2012.11.043 [arXiv:1209.5984 [hep-ph]].
- [17] I. Gogoladze, B. He, A. Mustafayev, S. Raza and Q. Shafi, *JHEP* **1405**, 078 (2014) doi:10.1007/JHEP05(2014)078 [arXiv:1401.8251 [hep-ph]].
- [18] A. Elsayed, S. Khalil and S. Moretti, *Phys. Lett. B* **715**, 208 (2012) doi:10.1016/j.physletb.2012.07.066 [arXiv:1106.2130 [hep-ph]].
- [19] S. Khalil and C. S. Un, *Phys. Lett. B* **763**, 164 (2016) doi:10.1016/j.physletb.2016.10.035 [arXiv:1509.05391 [hep-ph]].
- [20] T. Li, S. Raza and X. C. Wang, *Phys. Rev. D* **93**, no. 11, 115014 (2016) doi:10.1103/PhysRevD.93.115014 [arXiv:1510.06851 [hep-ph]].
- [21] Y. Hicyilmaz, M. Ceylan, A. Altas, L. Solmaz and C. S. Un, *Phys. Rev. D* **94**, no. 9, 095001 (2016) doi:10.1103/PhysRevD.94.095001 [arXiv:1604.06430 [hep-ph]].
- [22] I. Gogoladze, F. Nasir and Q. Shafi, *Int. J. Mod. Phys. A* **28**, 1350046 (2013) doi:10.1142/S0217751X13500462 [arXiv:1212.2593 [hep-ph]].
- [23] I. Gogoladze, F. Nasir and Q. Shafi, *JHEP* **1311**, 173 (2013) doi:10.1007/JHEP11(2013)173 [arXiv:1306.5699 [hep-ph]].
- [24] L. Calibbi, T. Li, A. Mustafayev and S. Raza, *Phys. Rev. D* **93**, no. 11, 115018 (2016) doi:10.1103/PhysRevD.93.115018 [arXiv:1603.06720 [hep-ph]].
- [25] I. Gogoladze, A. Mustafayev, Q. Shafi and C. S. Un, *Phys. Rev. D* **94**, no. 7, 075012 (2016) doi:10.1103/PhysRevD.94.075012 [arXiv:1609.02124 [hep-ph]].
- [26] Porod, W. *Comput. Phys. Commun.* **2003**, *153*, 275.
- [27] Porod, W. and Staub, F. *Comput. Phys. Commun.* **2012** *183*, 2458.
- [28] Staub, F. **2008**, *Preprint arXiv:0806.0538*.
- [29] Staub, F. *Comput. Phys. Commun.* **2011** *182*, 808.
- [30] Hisano, J.; Murayama, H.; and Yanagida, T. *Nucl. Phys. B* **1993** *402*, 46.
- [31] Chkareuli, J. L.; and Gogoladze, I. G. *Phys. Rev. D* **1998** *58*, 055011.
- [32] T. E. W. Group [CDF and D0 Collaborations], **2009**, *Preprint arXiv:0903.2503*.
- [33] Gogoladze, I.; Khalid, R.; Raza S.; and Shafi Q. *JHEP* **2011**, *1106*, 117.
- [34] Gogoladze, I.; Shafi, Q.; and Un, C. S. *JHEP* **2012** *1208*, 028.

- [35] Adeel Ajaib, M.; Gogoladze, I.; Shafi, Q.; and Un, C. S. *JHEP* **2013** 1307, 139.
- [36] Ibanez, L. E.; and Ross, G. G. *Phys. Lett. 110B* **1982** 215.
- [37] Inoue, K.; Kakuto, A.; Komatsu, H.; and Takeshita S., *Prog. Theor. Phys.* **1982** 68, 927.
- [38] Ibanez, L. E. *Phys. Lett.* **1982** 118B, 73.
- [39] Ellis, J. R.; Nanopoulos D. V.; and Tamvakis, K. *Phys. Lett.* **1983** 121B, 123.
- [40] Alvarez-Gaume, L.; Polchinski, J.; and Wise, M. B. *Nucl. Phys. B* **1983** 221, 495.
- [41] Nakamura, K. *et al.* [Particle Data Group Collaboration], *J. Phys. G* **2010** 37, 075021.
- [42] Belanger, G.; Boudjema, F.; Pukhov, A.; and Singh, R. K. *JHEP* **2009** 0911, 026.
- [43] Baer, H.; Kraml, S.; Sekmen, S.; and Summy, H. *JHEP* **2008** 0803, 056.
- [44] Olive, K. A. *et al.* [Particle Data Group Collaboration], *Chin. Phys. C* **2014** 38, 090001.
- [45] Aaij, R. *et al.* [LHCb Collaboration], *Phys. Rev. Lett.* **2013** 110, no. 2, 021801.
- [46] Amhis, Y. *et al.* [Heavy Flavor Averaging Group Collaboration], **2012**, *Preprint arXiv:1207.1158*.
- [47] Asner, D. *et al.* [Heavy Flavor Averaging Group Collaboration], **2010** , *Preprint arXiv:1010.1589*.
- [48] The ATLAS collaboration, *ATLAS-CONF-2015-067* **2015**.
- [49] J. Glatzer, PoS TOP **2015**, 014 (2016).